22. M. Boutros *et al.*, *Science* **303**, 832 (2004).
23. M. Ashburner *et al.*, *Genetics* **153**, 179 (1999).
24. M. K. Kerr, G. A. Churchill, *Proc. Natl. Acad. Sci. U.S.A.* **98**, 8961 (2001).
25. S. Richards *et al.*, in preparation.
26. W. Bender, B. Weiffenbach, F. Karch, M. Peifer, *Cold Spring Harbor Symp. Quant. Biol.* **50**, 173 (1985).
27. W. Bender, D. P. Fitzgerald, *Development* **129**, 4923 (2002).
28. H. D. Lipshitz, D. A. Peattie, D. S. Hogness, *Genes Dev.* **1**, 307 (1987).
29. M. D. Adams *et al.*, *Science* **287**, 2185 (2000).
30. S. Misra *et al.*, *Genome Biol.* **3**, RESEARCH0083 (2002).
31. C. Burge, S. Karlin, *J. Mol. Biol.* **268**, 78 (1997).
32. A. A. Salamov, V. V. Solovyev, *Genome Res.* **10**, 516 (2000).
33. M. Hild *et al.*, *Genome Biol.* **5**, R3 (2003).
34. G. Halasz *et al.*, unpublished data.
35. V.S. was supported by NASA Center for Nanotechnology, NASA Fundamental Biology Program, and NASA Biomolecular Systems Research Program (contract NAS2-99092). H.J.B. was partly supported by grant P20LM007276-01 from NIH. M.v.B. was supported by grant BMI 050.50.201 from the Netherlands Organization for Scientific Research (NWO). G.H. was supported by NIH training grant T32GM008224-17. C.M. was supported by an NSF Graduate Student Fellowship. This work was supported by grants to K.P.W. and H.J.B. from the Human Frontier Science Program and to K.P.W. from the Yale Genomics and Proteomics Initiative, the NIH National Human Genome Research Institute, and the W. M. Keck Foundation. Thanks to S. Schaeffer for providing syntenic block coordinates and F. Aoki for help with the probe design. The GSE accession number is GSE 1761.

Supporting Online Material
www.sciencemag.org/cgi/content/full/306/5696/655/DC1
Materials and Methods
SOM Text
fig. S1

9 June 2004; accepted 20 September 2004

REPORTS

Quantum-to-Classical Transition with Single-Photon–Added Coherent States of Light

Alessandro Zavatta, Silvia Viciani, Marco Bellini*

Single-photon–added coherent states are the result of the most elementary amplification process of classical light fields by a single quantum of excitation. Being intermediate between a single-photon Fock state (fully quantum-mechanical) and a coherent (classical) one, these states offer the opportunity to closely follow the smooth transition between the particle-like and the wavelike behavior of light. We report the experimental generation of single-photon–added coherent states and their complete characterization by quantum tomography. Besides visualizing the evolution of the quantum-to-classical transition, these states allow one to witness the gradual change from the spontaneous to the stimulated regimes of light emission.

A coherent state $|\alpha\rangle$ is the closest analog to a classical light field and exhibits a Poisson photon number distribution with an average photon number $|\alpha|^2$. Coherent states have relatively well-defined amplitude and phase, with minimal fluctuations permitted by the Heisenberg uncertainty principle. On the contrary, a Fock state $|n\rangle$ is strictly quantum-mechanical and contains a precisely defined number (n) of quanta of field excitation, hence its phase is completely undefined.

Photon-added coherent states (*1*) are the result of successive elementary one-photon excitations of a classical coherent field, and they occupy an intermediate position between the Fock and the coherent states. They are obtained by repeated (m times) application of the photon creation operator $\hat{a}^\dagger$ on a coherent state ($|\alpha,m\rangle = k_{\alpha,m}\ \hat{a}^{\dagger m}|\alpha\rangle$, $k_{\alpha,m}$ being a normalization constant and m an integer) and reduce to the limit Fock or coherent states for $\alpha \to 0$ or $m \to 0$, respectively. Quite differently from the so-called displaced Fock states, where a coherent state is used to displace a number state [for example, by mixing the two fields upon a highly reflecting beam splitter (*2*)], photon-added coherent states can be roughly viewed as obtained from the displacement of a coherent state operated by a Fock state. Indeed, one easily finds that all the $|n\rangle$ terms with $n < m$ are missing in the expansion of the states $|\alpha,m\rangle$ in the Fock basis, and that all the elements of the corresponding density matrix are essentially displaced toward higher indices $\rho_{i,j} \to \rho_{i+m,j+m}$, leaving all the elements with $i,j < m$ void.

In the case of a single quantum of field excitation ($m = 1$), the single-photon–added coherent states (SPACSs) read as

$$|\alpha, 1\rangle = \frac{\hat{a}^\dagger|\alpha\rangle}{\sqrt{1+|\alpha|^2}} \qquad (1)$$

Unlike the operation of photon annihilation, which maps a coherent state into another coherent state (that is, a classical field into another classical field), a single-photon excitation of a coherent state changes it into something quite different. In general, the application of the creation operator $\hat{a}^\dagger$ changes a completely classical coherent state into a quantum state with a varying degree of nonclassicality that becomes more evident the smaller the initial amplitude of the $|\alpha\rangle$ state. In the extreme case of an initial vacuum state $|0\rangle$, a single excitation event transforms it into the very nonclassical single-photon Fock state $|1\rangle$, which exhibits negative values of the Wigner function (*3*, *4*). The Wigner function is a quasi-probability distribution (*5*–*7*), which fully describes the state of a quantum system in phase space (either the position-momentum space for an harmonic oscillator or, equivalently, the space spanned by two orthogonal quadratures of the electromagnetic field for a single-mode state of light, as in this case) in the same fashion as a probability distribution (nonnegative by definition) characterizes a classical system. The negativity of the Wigner function is indeed a good indication of the highly nonclassical character of the state (Fig. 1).

We report the experimental generation of SPACSs and their complete tomographic analysis, which unveils the nonclassical features associated with the excitation of a classical coherent field by a single light quantum.

Parametric down-conversion in a nonlinear crystal is the basis for the production of the desired states (Fig. 2). Here one high-energy pump photon can annihilate into two photons that obey the global energy and momentum conservation laws and thus have lower energies and are normally emitted into symmetrically oriented directions, also called the signal and idler modes. When no other field is injected in the crystal, spontaneous parametric down-conversion takes place, starting from the input vacuum field, and pairs of entangled photons with random (but mutually correlated) phases are produced. In order to generate SPACSs, one has to inject a seed

Istituto Nazionale di Ottica Applicata, Largo Enrico Fermi, 6, I-50125, Florence, Italy; European Laboratory for Nonlinear Spectroscopy (LENS) and Department of Physics, University of Florence, I-50019 Sesto Fiorentino, Florence, Italy.

*To whom correspondence should be addressed. E-mail: bellini@ino.it

coherent field $|\alpha\rangle$ into the signal mode of the parametric amplifier, and the conditional preparation of the target state takes place every time that a single photon is detected in the correlated idler mode. If the parametric gain is kept sufficiently low, which is always the case in our experimental situation, the final output state can be approximated as

$$|\psi\rangle \approx (1+g\hat{a}_s^\dagger \hat{a}_i^\dagger)|\alpha\rangle_s|0\rangle_i = |\alpha\rangle_s|0\rangle_i + g\hat{a}_s^\dagger|\alpha\rangle_s|1\rangle_i \quad (2)$$

(where g is a gain constant with $|g| \ll 1$), and the output signal mode will contain the original coherent state most of the times, except for the few cases when the state $|1\rangle_i$ is detected in the idler output mode; these relatively rare detection events project the signal state into the SPACS $|\alpha,1\rangle_s$ (Fig. 2B), which corresponds to the stimulated emission of one photon in the same mode of $|\alpha\rangle$. The absence of a seed coherent field leaves with the usual expression for the spontaneous process, so that, by studying the evolution of the quantum state while the amplitude α gradually increases from zero, one can actually witness the smooth transition from the spontaneous to the stimulated regimes of light emission, with the transformation of an initial purely quantum state (the single-photon Fock state) into a classical coherent one. This is accompanied by the birth of a well-defined phase and can be described in more visual terms as the transition from the particlelike to the wavelike behaviors of the electromagnetic field.

The same state as described by Eq. 2 has recently been generated (*8*) to produce arbitrary superpositions of zero- and one-photon states. In that case, however, the conditioning was performed upon the detection of a single photon in the same mode $|1\rangle_s$ of the input coherent state, so that the final state was completely different from the ones investigated here and, for low α values, of the form $(\alpha|0\rangle_i + g|1\rangle_i)$. The injection of a single photon instead of a coherent state as a seed for conditional parametric amplification has also been investigated (*9*) and experimentally demonstrated (*10*, *11*) with the amplification to the $|2\rangle_s$ Fock state in the context of quantum cloning.

The primary light source for the experiment is a mode-locked laser whose pulses are frequency-doubled to become the pump for degenerate parametric down-conversion in a type-I beta-barium borate (BBO) crystal. In this configuration, the output photons share the same linear polarization and exactly the same wavelength, corresponding to twice that of the pump. In order to nonlocally select a pure state on the signal channel, idler photons undergo narrow spatial and frequency filtering before being detected by a single-photon counting module (*12*–*15*). The weak seed coherent state $|\alpha\rangle$ is obtained by controlled attenuation of a small portion of the laser emission, which is fed into the signal mode of the nonlinear crystal and is then directed to a 50% beam splitter. Here it is overlapped with a second (intense) coherent state (again obtained from a portion of the original laser pulses), which is spatially and temporally matched to the conditionally prepared SPACS and serves as the local oscillator (LO) for homodyne measurements, which are performed with a recently developed high-frequency time-domain technique (*4*, *16*, *17*).

Balanced homodyne detection (*18*–*20*) allows the measurement of the electric field quadratures of an unknown state as a function of the relative phase θ imposed between such a state and the reference LO. By performing a series of homodyne measurements on equally prepared states, it is possible to obtain the probability distributions $p(x,\theta)$ of the quadrature operator $\hat{x}_\theta = \frac{1}{2}\left(\hat{a}^\dagger e^{i\theta} + \hat{a}e^{-i\theta}\right)$ and, given a sufficient number of quadrature distributions for different values of θ, one is able to reconstruct the density matrix elements and the Wigner function of the field state under study (*7*, *17*).

Figure 3 shows a sequence of reconstructed Wigner functions for increasing values of the seed coherent field amplitude α. The first one (Fig. 3A), obtained with a blocked input, corresponds to the single-photon Fock state (*3*, *4*). Because of the finite efficiency (measured to be about 59% in the present set of measurements) in the detection apparatus, a significant mixture with the vacuum state is present, which clearly allows classically impossible negative values to be reached around the center of the circularly symmetric (because of the undefined value of the phase)

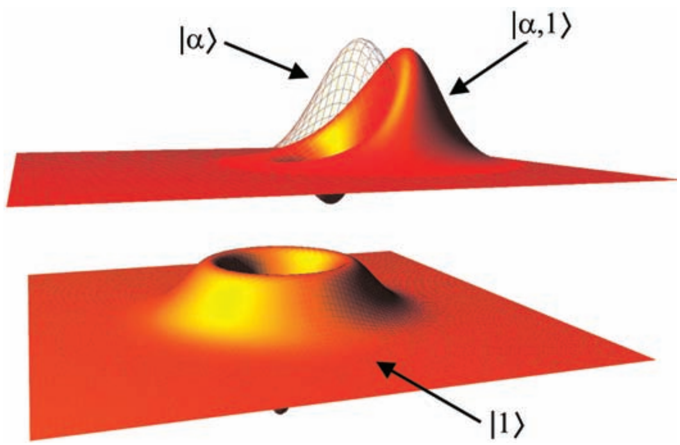

Fig. 1. Theoretical Wigner functions for some of the quantum states of light discussed in the text. Upper surface, SPACS $|\alpha,1\rangle$; wire-frame surface, original unexcited coherent state $|\alpha\rangle$; lower surface, single-photon Fock state $|1\rangle$. The horizontal plane coordinates represent two orthogonal quadratures of the field. The single-photon Wigner function is centered at the origin of the phase space. A value of $|\alpha|^2 = 1$ is used.

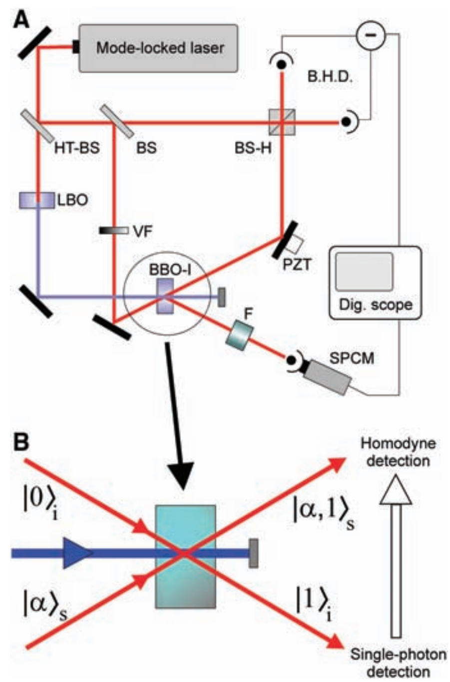

Fig. 2. Experimental apparatus and conceptual scheme for the conditional SPACS preparation. (**A**) Picosecond-duration pulses at 786 nm and at a repetition rate of 82 MHz from a mode-locked Ti:sapphire laser are split by a high-transmission (HT-BS) and a 50% (BS) beam splitter to serve as (i) the pump for spontaneous parametric down-conversion in a 3-mm-thick, type-I BBO crystal after frequency doubling in lithium triborate (LBO) crystal; (ii) the seed coherent field $|\alpha\rangle$, after proper attenuation by variable filters (VF); (iii) the local oscillator field for balanced homodyne detection (B.H.D.) after mixing with the investigated states in another 50% beam splitter (BS-H). F is a combination of spectral and spatial filters constituted by a pair of etalon interference filters with a narrow (50 GHz) spectral width, and by a single-spatial–mode optical fiber directly connected to a single-photon counting module (SPCM). PZT is a piezoelectric transducer used to vary the relative phase between the SPACS and the LO. Additional optics and computer-controlled optical delay lines to adjust the synchronization of the different pulses are not shown here for the sake of clarity. (**B**) The conditional preparation of a SPACS takes place whenever a "click"' is registered on the single-photon detector placed in the output idler mode. Each of these detection events triggers the acquisition in the balanced homodyne detector analyzing the output signal mode (*17*).

distribution. When the coherent seed is initially switched on at very low intensity ($|\alpha|^2 \approx 0.09$; that is, an average of less than one photon every 10 pulses), the Wigner function starts to lose its circular symmetry while moving away from the origin because of the gradual appearance of a defined phase, but it still exhibits an evident nonclassical nature, as indicated by its partial negativity (Fig. 3B). For increasing seed amplitudes, negativity is gradually lost (Fig. 3C) and the ringlike wings in the distribution start to disappear, making it more and more similar to the Gaussian typical of a classical coherent field (Fig. 3, C and D). Even at relatively high input amplitude, the Wigner distribution for the SPACS $|\alpha,1\rangle$ clearly shows the effect of the one-photon excitation as compared to the corresponding, slightly displaced, unexcited $|\alpha\rangle$ state (Fig. 3D).

Although the SPACS Wigner function eventually becomes entirely positive for sufficiently high values of the seed amplitude, the excitation of an otherwise classical coherent state by a single photon leaves a measurable mark of nonclassicality in the field quadrature statistics (*1*). In particular, whereas the original coherent state has equal fluctuations in the different quadratures independently from its amplitude, the one-photon–excited state exhibits a smaller uncertainty (a squeezing) in one of the quadratures and larger fluctuations in the orthogonal one. One can interpret this as a reduction in the intensity noise associated with the excitation by a perfectly defined number of quanta, which also increases the phase noise because of the lack of phase information intrinsic to Fock states. Whereas Fig. 4 clearly shows the amount of maximum quadrature squeezing for different values of the coherent seed amplitude, the effect on the intensity and phase noise is also evident from Figs. 1 and 3C. Here the reduced intensity fluctuations appear in the decreased width along the radial direction, whereas the increase in the phase noise is indicated by the appearance of the ringlike wings along the tangential direction of the Wigner distribution.

The ability to experimentally investigate the elementary action of the bosonic creation operator on a classical state is of interest both as a tool to take a closer look at such fundamental events in quantum physics and as a starting point for the investigation of the fuzzy border that separates the quantum and classical regimes of light behavior, with natural extensions toward even more "exotic" quantum entities, such as Schroedinger's cat states (*21*).

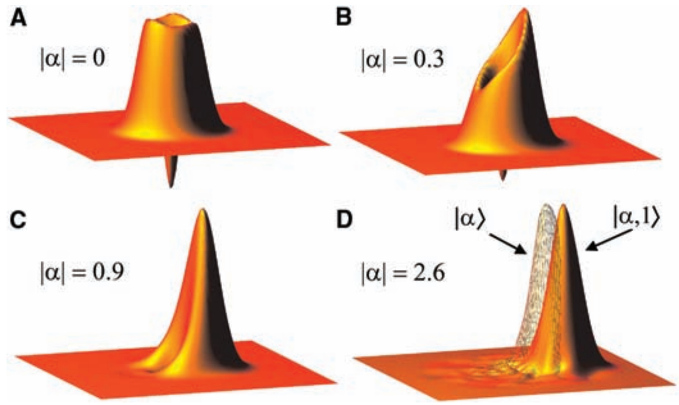

Fig. 3. Experimental Wigner functions for the SPACS. (**A**) Reconstructed Wigner function for the single-photon Fock state obtained without injection. (**B** to **D**) Same, but with an input coherent field of increasing amplitude. In (D), the reconstructed Wigner function for both the SPACS and the unexcited seed coherent state (wire-frame surface) are shown.

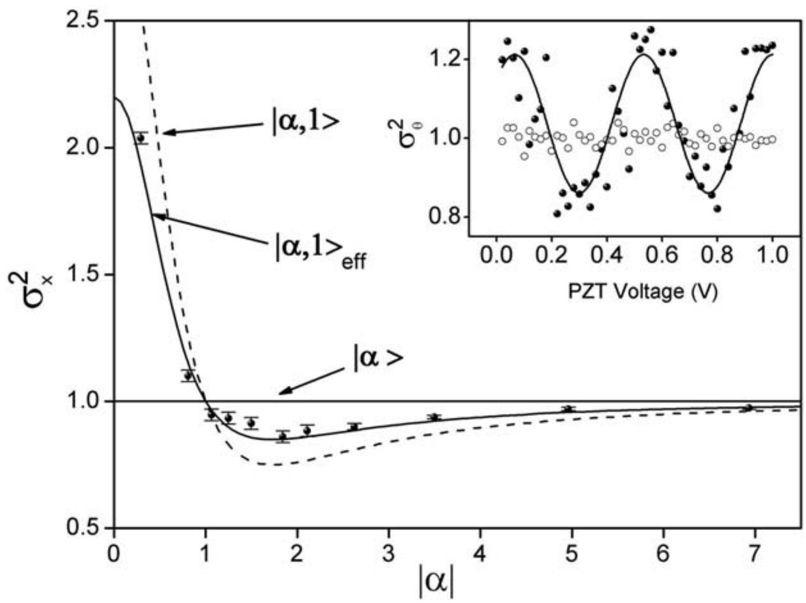

Fig. 4. Experimental squeezing data. Data points represent the variance in the SPACS field quadrature x_θ, which exhibits the maximum squeezing factor (about 15% for $|\alpha|$ between 1.5 and 2) normalized to the fluctuations of the coherent state $|\alpha\rangle$ (horizontal solid line). The dashed curve represents the theoretical prediction for a pure SPACS, whereas the solid one is calculated by taking into account the experimental detection efficiency. The measured variances for the different quadratures as a function of the phase θ (controlled by the PZT voltage) are shown in the inset for the states $|\alpha,1\rangle$ (solid circles) and $|\alpha\rangle$ (open circles) with $|\alpha| \approx 1.8$.

References and Notes

1. G. S. Agarwal, K. Tara, *Phys. Rev. A* **43**, 492 (1991).
2. A. I. Lvovsky, S. A. Babichev, *Phys. Rev. A* **66**, 011801 (2002).
3. A. I. Lvovsky *et al.*, *Phys. Rev. Lett.* **87**, 050402 (2001).
4. A. Zavatta, S. Viciani, M. Bellini, *Phys. Rev. A*, in press (e-print available at http://arxiv.org/abs/quant-ph/0406090).
5. L. Mandel, E. Wolf, *Optical Coherence and Quantum Optics* (Cambridge Univ. Press, Cambridge, 1995).
6. D. F. Walls, G. J. Milburn, *Quantum Optics* (Springer-Verlag, Berlin, 1994).
7. U. Leonhardt, *Measuring the Quantum State of Light* (Cambridge Univ. Press, Cambridge, 1997).
8. K. J. Resch, J. S. Lundeen, A. M. Steinberg, *Phys. Rev. Lett.* **88**, 113601 (2002).
9. Z. Y. Ou, L. J. Wang, L. Mandel, *J. Opt. Soc. Am. B* **7**, 211 (1990).
10. F. De Martini, V. Mussi, F. Bovino, *Opt. Commun.* **179**, 581 (2000).
11. A. Lamas-Linares, C. Simon, J. C. Howell, D. Bouwmeester, *Science* **296**, 712 (2002).
12. Z. Y. Ou, *Quantum Semiclass. Opt.* **9**, 599 (1997).
13. T. Aichele, A. I. Lvovsky, S. Schiller, *Eur. Phys. J. D* **18**, 237 (2002).
14. M. Bellini, F. Marin, S. Viciani, A. Zavatta, F. T. Arecchi, *Phys. Rev. Lett.* **90**, 043602 (2003).
15. S. Viciani, A. Zavatta, M. Bellini, *Phys. Rev. A* **69**, 053801 (2004).
16. A. Zavatta, M. Bellini, P. L. Ramazza, F. Marin, F. T. Arecchi, *J. Opt. Soc. Am. B* **19**, 1189 (2002).
17. Materials and methods are available as supporting material on *Science* Online.
18. S. Reynaud, A. Heidmann, E. Giacobino, C. Fabre, in *Progress in Optics*, E. Wolf, Ed. (Elsevier, Amsterdam, 1992), vol. 30, pp. 1–85.
19. G. Breitenbach, S. Schiller, J. Mlynek, *Nature* **387**, 471 (1997).
20. D. T. Smithey, M. Beck, M. G. Raymer, A. Faridani, *Phys. Rev. Lett.* **70**, 1244 (1993).
21. A. Montina, F. T. Arecchi, *Phys. Rev. A* **58**, 3472 (1998).

22. We thank F. T. Arecchi for helpful comments and for a critical reading of the manuscript. This work was performed in the frame of the "Spettroscopia laser e ottica quantistica" project of the Department of Physics of the University of Florence, with the support of the Italian Ministry of University and Scientific Research (MIUR) under the FIRB contract "Microdispositivi fotonici in Niobato di Litio."

Supporting Online Material
www.sciencemag.org/cgi/content/full/306/5696/660/DC1
Materials and Methods
References

23 July 2004; accepted 15 September 2004